Chemistry & Biology *13*, 251–259, March 2006 DOI 10.1016/j.chembiol.2005.12.010

Multivalent Fertilinβ Oligopeptides: The Dependence of Fertilization Inhibition on Length and Density

Keith A. Baessler,[1] Younjoo Lee,[2] Kenny S. Roberts,[2] Nicole Facompre,[2] and Nicole S. Sampson[2,*]
[1] Biochemistry and Structural Biology Graduate Program
[2] Department of Chemistry
Stony Brook University
Stony Brook, New York 11794

Summary

The sperm protein fertilinβ, a member of the ADAM family of proteins, is implicated in sperm-egg binding in all mammals studied to date. Multivalent inhibitors containing the three amino acid binding sequence of fertilinβ, ECD, have been shown previously to be more effective inhibitors of fertilization than their monovalent counterparts. Here, we probed sperm-egg interactions with ruthenium-catalyzed ring-opening metathesis polymers that contained from 3 to 70 ECD pharmacophores in densities ranging from 10% to 100%. Evaluation of the polymer potencies, and synthesis of a triblock copolymer from two building blocks, revealed that two multivalent contacts are sufficient for maximal inhibition, and that the distance between ECD pharmacophores required is 7–9 monomers spanning 4–5 nm. We conclude that inhibition requires recruitment of two receptors on the egg surface into an inhibitory complex.

Introduction

Fertilization of a mammalian oocyte by a single sperm is an extremely complex event. Many of the protein-protein and protein-carbohydrate interactions in the pathway are still unknown. The organization, localization, and binding properties of receptor-ligand complexes between sperm and egg still need to be characterized. Elucidation of the pathway and the mechanisms involved is critical for the design and synthesis of pharmaceuticals, which target population control and treat infertility. Sperm-egg recognition, binding, and fusion events are dictated by a variety of multivalent receptor-ligand contacts. Using ring-opening metathesis polymerization (ROMP), we have developed synthetic ligands that mimic the multivalent display of sperm protein fertilinβ [1]. Here, we demonstrate the value of ROMP chemistry for discerning the optimal fertilinβ ligand presentation.

Fertilinβ is located in the equatorial region of the sperm head and is involved in sperm binding to the egg plasma membrane during fertilization [2–5]. Fertilinβ is a member of the ADAM (*a d*isintegrin and *a m*etalloprotease domain) family of proteins [6]. A tripeptide, Glu-Cys-Asp (ECD), is the minimal recognition element necessary for the binding of fertilinβ to its egg receptor [7–10]. This recognition motif is taken from the sperm protein's disintegrin loop. Peptides containing the ECD motif inhibit sperm-egg adhesion in vitro [1, 7, 8, 11–13]. For example, the IC_{50} for inhibition of fertilization by the ECD monomer **1** is ~500 μM. Peptides containing this sequence have been assayed in a diverse range of species, and the peptides inhibit fertilization in all of them [7, 8, 12, 14–16]. Thus, ECD is a small pharmacophore around which inhibitors of fertilization may be designed.

Regardless of their length or flanking sequence, all monomeric ECD peptides are poor inhibitors. Knowing that multivalent display of ligands often improves their affinity [17–20], we developed multivalent presentations of the ECD ligand [1, 13, 21]. Liposomes presenting eight copies of the ECD ligand are 100-fold better inhibitors than the corresponding monomer [13, 21]. Polymers containing ten copies of the ECD motif, e.g., $\mathbf{2}_{10}$, show 50- to 70-fold increased inhibition over the corresponding monomer [1]. These are the highest potencies reported to date for an ECD inhibitor. Incorporation of a fluorophore into the probes established that the target of the polyvalent ECD inhibitors is on the surface of the egg, and not on the sperm surface [21, 22]. Previously, we synthesized an ^{125}I-labeled DECD peptide, which both inhibited fertilization, and photoaffinity-labeled integrin $\alpha_6\beta_1$ [23]. Several other laboratories have also reported integrin $\alpha_6\beta_1$ as being the receptor [12, 24, 25]. However, Myles and coworkers have established that mice with a conditional β_1 integrin knockout in the egg are fertile [26], and that α_6 null eggs are still fertilized by wild-type sperm [27]. Little information has been obtained about the differences of the egg surface proteome between the integrin knockout eggs and wild-type eggs because of the extraordinarily small amounts of protein material that may be obtained. Clearly, chemical methods that can be used to investigate the proteome are required. In this work, we advance ROMP of peptide-bearing monomers to define the optimal presentation of ECD ligands for future development of proteome probes that are of high affinity and that have useful handles for identification of cell surface receptors and coreceptors.

We employed ruthenium-catalyzed ROMP [28] for several reasons. Using ROMP, it is possible to prepare polymers of well-defined length. Ruthenium catalysts are very stable, readily available, and functional group tolerant. In addition, ROMP allows for the multivalent presentation of one or more functional groups along a polymer backbone. Monomer building blocks are constructed from strained cyclic alkenes—in our case, 5-norbornene-*exo*-carboxylic acid. The utility of ROMP is that one can easily manipulate the length of a polymer by varying the monomer:catalyst ratio. Moreover, the pharmacophore density of a polymer is readily adjusted by feeding two simple monomer building blocks, one a pharmacophore and one a spacer, to the catalyst in varying ratios. The pharmacophore and spacer may be mixed in a random fashion [29–31]. In this work, we take advantage of the living nature of the polymerization catalyst to prepare block copolymer. Thus, using one or two simple monomer building blocks and ROMP chemistry, a family of polymers may be generated to

*Correspondence: nicole.sampson@stonybrook.edu

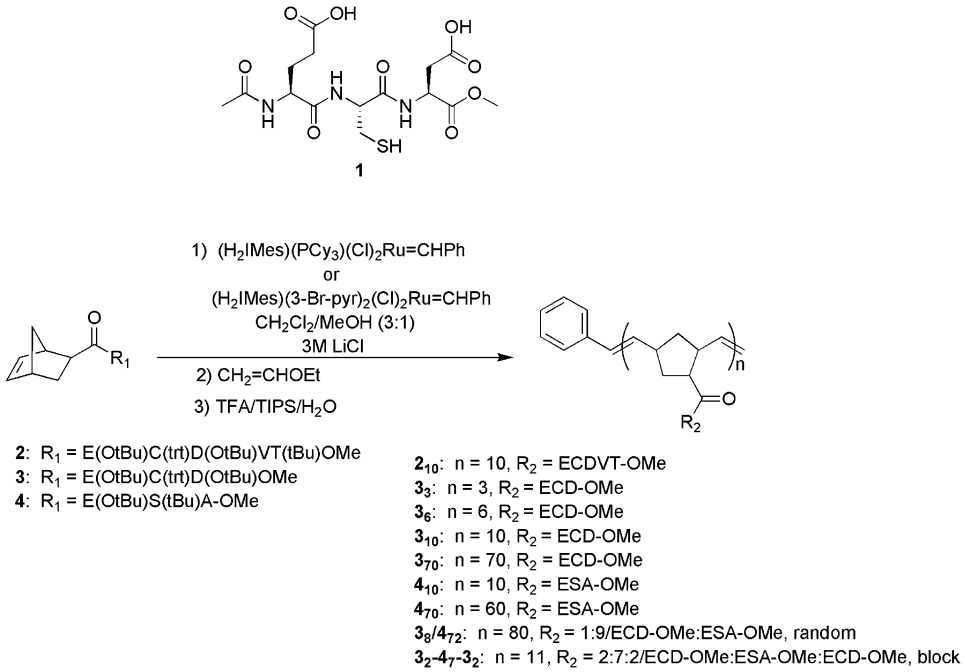

Figure 1. Polymers Synthesized by ROMP and Tested as Fertilization Inhibitors

The compound number refers to the structure of the ligand. The subscript to the compound number refers to the number of that specific monomer in the polymer. Refer to Figure 2 for a cartoon representation of the polymer structures.

determine the length and spacing requirements for maximal polymer affinity or avidity.

We synthesized a family of structurally diverse fertilinβ peptide polymers derived from **2_{10}** by using a combination of solution-phase peptide synthesis and ROMP to define the best inhibitor structure (Figure 1). Polymers **3_{10}**, **3_{70}**, **4_{10}**, **4_{70}**, **$3_8/4_{72}$**, **3_3**, **3_6**, and **3_2-4_7-3_2** were tested as inhibitors in a mouse in vitro fertilization assay. These polymers were chosen to present a diversity of size and densities to the egg. With their assay, we explored the role of inhibitor length and pharmacophore spacing. The chemical approach developed here is general and will be of use for exploring receptor-ligand interactions in many different biological systems.

Results

Synthesis of Polymers

The peptide monomers **3** and **4** were synthesized by using standard solution-phase procedures with t-butyl/trityl-based side chain protection and Fmoc/Cbz α-amino protection. Solution-phase methods were used in order to obtain large quantities of pure peptide for ROMP. Polymers were prepared by ROMP by using fully protected peptides and $(H_2IMes)(PCy_3)$ Cl_2Ru=CHPh or $(H_2IMes)(3\text{-Br-pyr})_2Cl_2Ru$=CHPh as the catalyst in dichloromethane/methanol (3/1) with 3 M LiCl to solubilize the polymer as previously described (Figure 1) [32]. Polymers were deprotected with a trifluoroacetic acid/water/triisopropylsilane cocktail and were precipitated with diethyl ether. They were reduced with tris(2-carboxyethyl)-phosphine, precipitated with dilute acid, and resuspended in aqueous ammonium hydroxide at pH 7 before use in assays. Isolated yields were 63%–95%. Integration of NMR spectra confirmed that the number of monomers incorporated into each polymer was the same as the initial monomer:catalyst ratio. Gel permeation chromatography (GPC) was used to analyze and monitor the molecular weight distribution of the polymer block intermediates in the synthesis of **3_2-4_7-3_2**. The synthetic precursors **$3_2'$** and **$3_2'$-$4_7'$** and product **$3_2'$-$4_7'$-$3_2'$** were analyzed with side chain protection intact (Figure 2). For each reaction, the disappearance of the monomer was monitored by TLC before addition of the subsequent monomer. Then, a portion of the polymerization reaction was quenched with ethylvinyl ether after each monomer addition for analytical purposes. The three protected polymers were analyzed by ^{1}H-NMR spectroscopy, and their monomer compositions corresponded to the monomers fed to the polymerization reaction. GPC of **$3_2'$**, **$3_2'$-$4_7'$**, and **$3_2'$-$4_7'$-$3_2'$** confirmed that none of the precursor block remained after addition of the subsequent monomer, and that the number-average molecular weights shifted as expected (Figure 2). The final triblock copolymer **$3_2'$-$4_7'$-$3_2'$** had a narrow polydispersity index of 1.21, consistent with a controlled, living polymerization.

Assay of Polymers

Polymers were assayed as inhibitors in a mouse in vitro fertilization assay. Sperm fusion was used as an endpoint to measure inhibition of sperm binding. Two measures of fertilization were calculated: fertilization rate (FR) and fertilization index (FI) [7]. The FR is the total number of eggs fertilized divided by the total number of eggs. The FI is the total number of sperm fused divided by the total number of eggs. Inhibitor concentrations were varied over at least a 400-fold range to determine their IC_{50}s by both FR and FI. Concentrations were considered both in peptide ligand and in polymer (Table 1). For example,

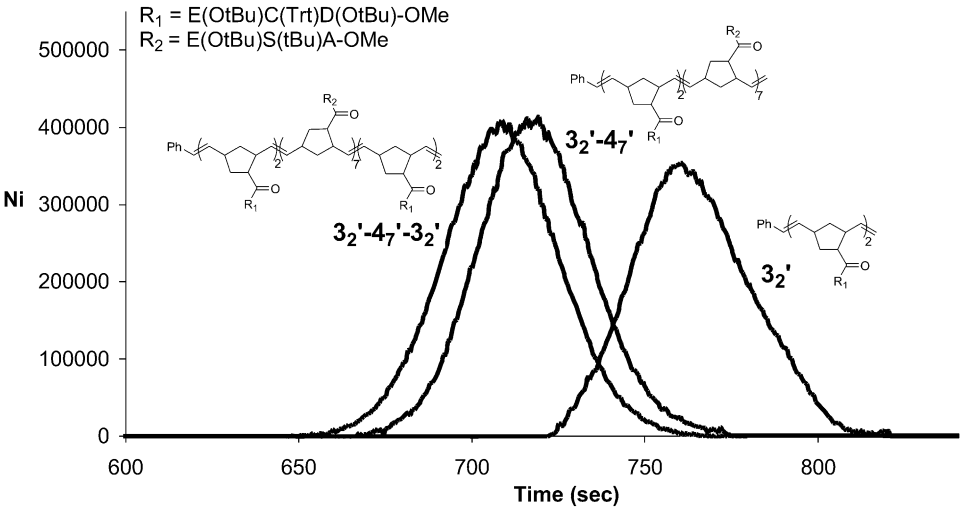

Figure 2. Gel Permeation Chromatography Characterization of Block Copolymer

Comparison of GPC-eluted peaks of $3_2'$, $3_2'$-$4_7'$, and $3_2'$-$4_7'$-$3_2'$ was performed by using a Phenogel column (5μ, 300 × 4.6 mm, linear mixed bed, 100–10^6 MW range) eluting with 0.3 ml/min 10% MeOH in CH_2Cl_2. Narrowly dispersed polystyrene standards were used to calibrate number-averaged molecular weight. Polymer $3_2'$ eluted at an apparent M_n of 3,372 (PDI: 1.18; expected MW: 1,812), polymer $3_2'$-$4_7'$ eluted at an apparent M_n of 10,840 (PDI: 1.18; expected MW: 5,673), and the triblock copolymer $3_2'$-$4_7'$-$3_2'$ has an apparent M_n of 15,013 (PDI: 1.21; expected MW: 7,382).

a 10 μM (in polymer) solution of 3_{10} contains 100 μM ECD ligand. Peptide ligand concentrations are useful for comparing the inhibition efficiencies of polymers containing different numbers of ligands.

Sperm Susceptibility to Polymers

Sperm were allowed to capacitate and acrosome react and were then treated with polymer and observed under a light microscope. The percentage of live, motile sperm remaining after 45 min was the same in control incubations and in 500 μM polymer incubations (70% ± 7% for 3_{10}, 76% ± 11% for 3_{70}, 74% ± 11% for 3_2-4_7-3_2, and 74% ± 8% for the control). Sperm were also incubated with 125 μM 3_2-4_7-3_2 for 45 min prior to insemination of eggs. In these experiments, the final concentration of 3_2-4_7-3_2 in the sperm-egg incubation buffer was below the IC_{50}. There was no difference in FR or FI with pretreated sperm compared to fertilization by control sperm that were incubated in buffer alone (Figure 3). Lastly, no inhibition was observed in the presence of 500 μM negative control polymers 4_{10} or 4_{70} (Table 1).

Discussion

Understanding protein-protein interactions in fertilization is of fundamental importance for elucidating the molecular display required for biological function. However, this biological system is not amenable to many methods typically used to probe protein interactions—for example, phage display or mutagenesis of intact egg proteins—because of the limited quantities of material available to study gametes in mammalian systems

Table 1. Polymer IC_{50}s for Inhibition of In Vitro Fertilization

Polymer	IC_{50} (μM) in Peptide by FI[a]	IC_{50} (μM) in Peptide by FR	IC_{50} (μM) in Polymer by FI	IC_{50} (μM) in Polymer by FR
1 (monomer)	>500[b]	>500[b]	n.a.[c]	n.a.
2_{10}	5.1 ± 1.4	5.8 ± 0.3	0.51 ± 0.14	0.58 ± 0.03
3_{10}	3.4 ± 0.3	3.2 ± 0.2	0.34 ± 0.03	0.32 ± 0.02
3_{70}	68 ± 11.1	99 ± 31	0.97 ± 0.16	1.4 ± 0.44
3_8/4_{72}	23 ± 5	80 ± 24	2.9 ± 0.7	10 ± 4
4_{10}	n.i.[d]	n.i.	n.i.	n.i.
4_{70}	n.i.[d]	n.i.	n.i.	n.i.
3_3	~500[e]	~500[e]	~167	~167
3_6	~500[f]	~500[f]	~83	~83
3_2-4_7-3_2	1.1 ± 0.3	5.5 ± 2.3	0.28 ± 0.08	1.4 ± 0.6

[a] FI (fertilization index) is the average number of fused sperm per egg. The average FI of the control was 1.93. FR (fertilization rate) is the percentage of eggs fertilized. The average FR of the control was 85.7%. A total of 200–300 eggs were assayed for each polymer in 8–10 independent experiments. IC_{50}s were calculated by a three parameter fit (GRAFIT software) by using the equation: percent fertilization = $(100 - b)/\{1 + ([I]/IC_{50})\}^s$, where b is the remaining percent fertilization after saturation with inhibitor, and s is the slope of the fit. Errors are reported as SEM.
[b] At 500 μM **1**, 29% (F.I.) and 32% (F.R.) were observed.
[c] n.a.: not applicable.
[d] n.i.: no inhibition. Negative control polymers 4_{10} and 4_{70} did not inhibit fertilization at 500 μM (peptide).
[e] At 500 μM 3_3 (peptide), the percent inhibition observed was 66 ± 9 (FI) and 58 ± 2 (FR).
[f] At 500 μM 3_6 (peptide), the percent inhibition observed was 57 ± 5 (FI) and 52 ± 4 (FR).

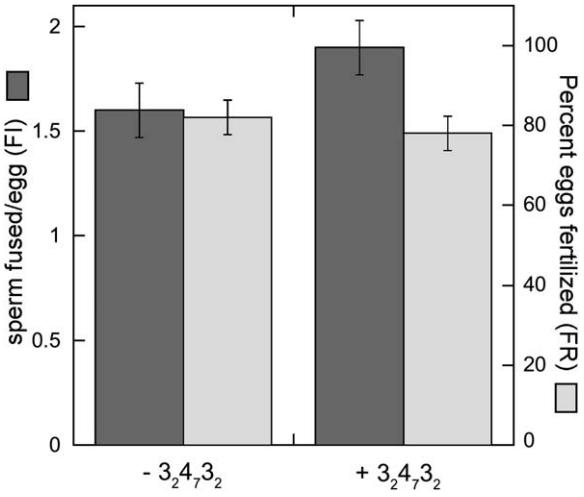

Figure 3. Assay of Sperm Susceptibility to Polymers

Sperm were incubated with 3_2-4_7-3_2 (125 μM in peptide) or M16 buffer for only 45 min prior to egg insemination (final 3_2-4_7-3_2 concentration was ~2 μM in peptide). The 3_2-4_7-3_2-pretreated sperm and control sperm fertilized eggs equally efficiently, as measured by both fertilization rate (FR) and fertilization index (FI), demonstrating that the polymer does not have an adverse affect on the sperm. A total of 60 eggs were used in 3 independent experiments. Errors are reported as standard error of measurement.

and the lack of cell culture models. We have developed ROMP chemistry in order to advance our understanding of fertilization with polymer probes.

Previously in our laboratory, we demonstrated that a norbornyl polymer displaying the peptide sequence ECDVT, 2_{10}, is a significantly more potent inhibitor of fertilization than a simple monomeric peptide [1]. The first step to optimize polymer structure was to simplify the ligand appended to the polymer backbone. We prepared and tested 3_{10} and compared its potency to that of 2_{10}. Inhibition by 3_{10} was equipotent to that of 2_{10} (Table 1). These results demonstrate that, as expected, removal of valine and threonine to shorten the ligand sequence to ECD did not impair inhibition. The polymer behaved similarly to 2_{10}. The shorter ligand improved solubility of the ROMP monomer precursors, as well as the polymer, and reduced the number of synthetic steps required.

In order to be certain that the inhibition observed was caused by the ECD binding motif, we prepared control polymers 4_{10} and 4_{70} with the mutant sequence ESA. We chose to mutate ECD rather than scramble it because two of the amino acids contain carboxylates. We were concerned that scrambling the peptide might not completely eliminate binding, and that multivalent presentation would restore significant inhibition. We chose to mutate cysteine and aspartate because mutagenesis work by White and coworkers [33] and Evans and coworkers [9] showed that these residues were critical for binding. We retained the glutamate residue for solubility reasons. No inhibition of fertilization by polymers 4_{10} and 4_{70} was observed at polymer concentrations of 50 and 8 μM, respectively. Thus, the inhibition by 3_{10} observed is due to a specific interaction of the ECD peptide with a cell surface molecule.

Previous work had demonstrated that fluorescently labeled polymer 2_{10} binds to the surface of the egg, and not the sperm surface [22]. We tested whether the inhibition observed could be due to deleterious effects of polymer upon sperm. Polymers that only contained ESA peptide substituants, e.g., 4_{10} and 4_{70}, showed no inhibition of fertilization. Incubation of sperm with ECD-containing polymers did not affect their motility or viability. Sperm pretreated with polymer 3_2-4_7-3_2 before insemination in M16 buffer were able to fertilize eggs normally (Figure 3). Therefore, treatment of sperm with our polymers does not affect sperm viability, motility, or penetrability. Targeting of the ECD polymers for the egg cell surface is responsible for inhibition.

A longer polymer should cluster many more receptors on the oocyte and have a statistical advantage that favors rebinding of ligand over dissociation; therefore, longer polymers should be a more potent sperm inhibitors. For example, in studying glycopolymer inhibition of hemagglutination, Kanai and coworkers have shown that inhibition potency (as measured on a per residue basis) saturates at a length of about 50 residues [18]. Inhibition potency does not decrease as the polymer length increases beyond the length required to span binding sites as would be expected if only chelation were important [18]. Hence, we synthesized polymer 3_{70}, which contained approximately 70 ECD ligands, and polymer $3_8/4_{72}$. Polymer $3_8/4_{72}$ was approximately the same length as polymer 3_{70}, but only 10% of the peptides presented (randomly) were the ECD ligand; the remainder were the ESA mutant sequence. To our surprise, we observed that the longer polymers showed decreased inhibition potency compared to 3_{10} when compared on the basis of peptide concentration (Table 1). When compared on the basis of polymer concentration, 3_{10} and 3_{70} are essentially equipotent, and $3_8/4_{72}$ is less effective.

Previous investigations had demonstrated that if the cysteine residue of the ECD sequence is protected as a disulfide, no inhibition is observed [8, 10]. We investigated the rate of thiol oxidation in the polymers under the conditions of the in vitro fertilization assay. If significant oxidation of the polymer thiols were to occur faster in the longer polymers, their potency would be reduced compared to the shorter polymers. We measured reduced thiol concentration as a function of time by using 5,5′-dithiobis(2-nitrobenzoic acid) [34] in M16 buffer at 37°C. For all of the polymers, less than 20% of the thiols were oxidized over the 45 min incubation period of the assay, and the oxidation rate of 3_{10} did not differ significantly from the oxidation rates of 3_{70} and $3_8/4_{72}$.

We concluded that increasing the number of ligands presented and/or increasing the distance between ligands did not improve inhibitor potency. Our data imply that chelation of the receptor is more important than statistical factors favoring ligand rebinding. A polymer length of ten represented the maximum length required for efficient inhibition. When modeled in the most extended backbone configuration (*trans*-syndiotactic), the distance spanned by 3_{10} is at most 5.3 nm. We next sought to determine the minimum length of polymer required for inhibition.

We synthesized fully substituted ECD ligand 3-mers and 6-mers. Polymers 3_3 and 3_6 were both poor inhibitors, and they showed no more potency than the ECD

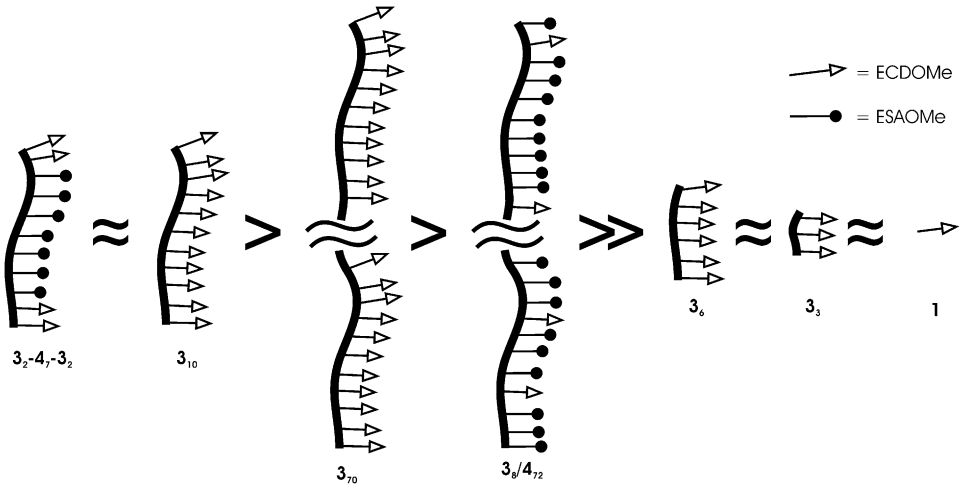

Figure 4. Relative Potencies of Fertilinβ Polymers When Compared on the Basis of Peptide Ligand Concentration

monomer **1**. These results indicated that multivalency was required for effective binding and inhibition, and that the 3-mer and 6-mer did not have sufficient length to span the distance between binding sites of two adjacent receptors. In the most extended configuration, 3_6 can, at most, span 3 nm.

The poor inhibition of fertilization by polymer 3_6 implied that the potency of 3_{10} was due to the ligation of the terminal ECD moieties, and that the internal ECD peptides did not engage receptor binding sites. The living nature of the ROMP polymerization allows for the sequential addition of monomer building blocks to the growing polymer chain. We took advantage of this polymer property to construct 3_2-4_7-3_2, which contained, on average, two ECD ligands at either terminus separated by a 7-mer spacer comprised of biologically inactive ESA peptides. The block nature of the polymer was verified by gel permeation chromatography (GPC) analysis of $3_2'$-$4_7'$-$3_2'$ as well as the monoblock and diblock precursors (Figure 2). There were no low molecular weight shoulders on the $3_2'$-$4_7'$-$3_2'$ peak, confirming that the polymerization was living, and that the intact triblock polymer had been prepared.

The inhibition potency of polymer 3_2-4_7-3_2 was equal to that of polymer 3_{10} in polymer concentration, and it was slightly better when compared on the basis of peptide concentration. We conclude that the internal ECD ligands in polymer 3_{10} are not required for binding or inhibition (Figure 4). The distance between ECD ligands on an extended 9-mer is ~4.7 nm, and on an extended 10-mer, it is ~5.3 nm, indicating that the distance between receptor binding sites can be no greater than 5 nm (Figure 5). Typically, membrane protein receptors are 2–3 nm in diameter. Based on the ineffective inhibition observed with polymer 3_6, fertilinβ receptor binding sites are more than 3 nm apart. Taken together, our polymers appear to engage the egg surface receptor in a bivalent fashion (Figure 5).

Our results are analogous to other systems in which bivalent inhibitors show high selectivity and affinity. For example, Portoghese and coworkers designed bivalent ligands for the opioid receptors [35]. Their results are consistent with a model in which two receptors are recruited into van der Waals contact, ~3 nm apart. Potent proteasome inhibitors have been designed by using a similar strategy. Moroder and coworkers [36, 37] synthesized inhibitors containing two Arg-Leu-Arg peptides spaced by a 6.5 nm polyethylene glycol linker. The bivalent inhibitor was 124-fold more potent than the monomeric peptide. Potent inhibition required a linker that was flexible and long enough to span the distance between the active β subunits of the proteosome.

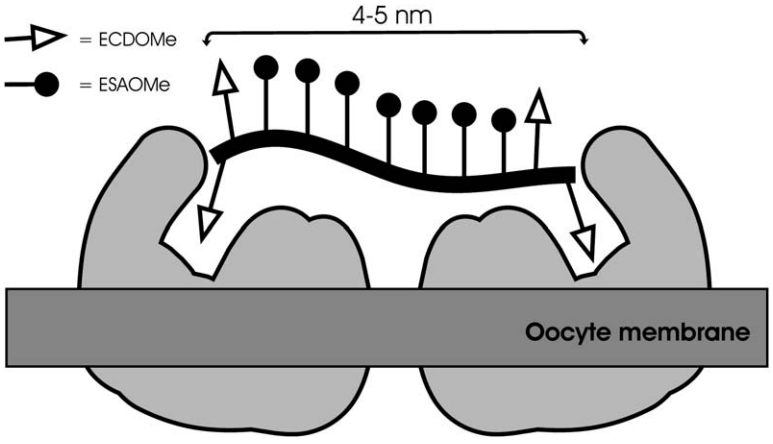

Figure 5. Proposed Model for Receptor-Polymer Binding

Our polymer assay results are consistent with a bivalent inhibition model like that of the opioid receptor or the proteosome. Using block synthesis of copolymers, we conclude that inhibition of fertilization by fertilinβ mimics requires recruitment of two receptors on the egg surface into an inhibitory complex. The recruitment of additional receptors with longer polymers does not enhance inhibition potency. These experiments establish the parameters for future polymer design and testing. The structural requirements defined here will be incorporated into future polymers that include tagging elements for probing the identity of egg surface fertilinβ receptors.

Significance

The mechanisms by which spermatozoa bind and fuse to the oocyte plasma membrane during mammalian fertilization are still unknown. In this work, we utilized the fertilinβ binding site peptide ECD to define the molecular structure required for optimal inhibition of in vitro fertilization, a measure of sperm-egg binding. Using two simple monomeric building blocks, a diverse series of polymers was synthesized by ring-opening polymerization (ROMP) of norbornene. We introduce block copolymer synthesis as a method by which to optimize polymer potency and to rapidly identify required spacer lengths. In our polymer series, the length of spacer between ECD pharmacophores and the numbers of ECD pharmacophores presented to the egg were varied. Polymers tested contained as few as 3 ECD ligands and as many as 70 ECD ligands. The most potent fertilinβ-derived inhibitor of fertilization to date is an 11-mer polymer that contains two ECD ligands at either terminus separated by seven spacer monomers. These results indicate that two ECD ligands bound to the egg surface separated by 4–5 nm are sufficient for maximal inhibition. Definition of the optimal polymer structure for inhibition now allows for the design of molecular probes to identify the egg cell surface members of the inhibitory complex.

Experimental Procedures

Materials

Amino acids and coupling agents used were purchased from Advanced Chem Tech. (Louisville, KY) or PerSeptive Biosystems (Framingham, MA). Solvents and chemical reagents were obtained from Fisher Scientific, Inc. (Springfield, NJ) or Sigma-Aldrich (Milwaukee, WI). Pregnant mare's serum gonadotropin (PMSG, #367222), hyaluronidase (#H3506), and Hoechst-33342, were purchased from Sigma-Aldrich, and human chorionic gonadotropin (hCG, #230734) was obtained through the National Hormone and Peptide Program, the National Institute of Diabetes and Digestive Kidney Diseases, and Dr. A.F. Parlow. $(H_2IMes)(PCy_3)Cl_2Ru{=}CHPh$ was purchased from Sigma-Aldrich (Milwaukee, WI). $(H_2IMes)(3\text{-}Br\text{-}pyr)_2Cl_2Ru{=}CHPh$ was prepared according to the literature [38]. CH_2Cl_2 was freshly distilled from CaH; CH_3OH and Et_2O, were used without further purification. LiCl was oven dried and stored over P_2O_5 before use. All reactions were carried out under an Ar atmosphere in oven-dried glassware unless otherwise specified. Moisture and oxygen-sensitive reagents were handled in an N_2-filled drybox. 5-Norbornene-*exo*-carboxylic acid was synthesized according to the literature [19].

General Methods

Analytical thin layer chromatography (TLC) was performed on precoated silica gel plates (60F254) and flash chromatography on silica gel-60 (230–400 mesh). TLC spots were detected by UV light and by staining with phosphomolybdic acid (PMA). Peptides were purified by flash column chromatography on silica gel-60. The purities of all peptide monomers were assessed by RPHPLC by using a Vydac C18 column. Gradient elution was performed at 1 ml/min with acetonitrile and water (both containing TFA, 0.1%). The purity of the polymers was assessed by aqueous-phase gel permeation chromatography (BioSep-SEC-S2000) by using 50 mM potassium phosphate (pH 7). Inova400, Inova500, and Inova600 MHz NMR spectrometers were used to perform NMR analysis, and spectra were recorded in $CDCl_3$ unless otherwise noted. ^{1}H-NMR spectra are reported as chemical shift in parts per million (multiplicity, coupling constant in Hz, integration). ^{1}H-NMR data are assumed to be first order. Copies of spectra are available in the Supplemental Data with this article online. The usual workup for peptide coupling reactions was three washes of the CH_2Cl_2 solution with 5% $NaHCO_3$, followed by three washes with 1 N HCl and drying of the CH_2Cl_2 over Na_2SO_4. After evaporation of solvent, the peptide product was purified by flash silica chromatography.

PMSG and hCG were resuspended in sterile PBS to 10 IU/100 μl. These solutions were stored at −20ºC. Hyaluronidase was resuspended in sterile water to a final concentration of 30 mg/ml and was stored at −20ºC. Hoechst-33342 was stored in the dark at 4ºC. All of the steps involving the use of Hoechst dye were performed with minimum exposure to light.

Fmoc-Cys(trt)Asp(OtBu)-OMe

H-Asp(OtBu)-OMe·HCl (16.69 mmol, 4.00 g), Fmoc-Cys(trt)-OH (18.36 mmol, 10.75 g), EDC·HCl (20.03 mmol, 3.83 g), and HOBt·hydrate (20.03 mmol, 3.07 g) were dissolved in 40 ml dry CH_2Cl_2 and cooled to 0ºC. DIEA (18.36 mmol, 3.25 ml) was added, and the reaction was stirred for 4 hr at room temperature. The usual workup and chromatography (acetone:CH_2Cl_2/1:20) yielded Fmoc-Cys(trt)Asp(OtBu)-OMe (12.7 g, 98%) as a white powder. ^{1}H-NMR (400 MHz) δ 7.74 (t, J = 7.6 Hz, 2), 7.57 (d, J = 4.8 Hz, 2H), 7.31 (m, 19H), 6.78 (d, J = 7.6 Hz, 1H), 5.01 (d, J = 6.8 Hz, 1H), 4.71 (m, 1H), 4.34 (m, 2H), 4.19 (t, J = 7.0 Hz, 1H), 3.76 (dd, J = 6.8, 6.8 Hz, 1H), 3.66 (s, 3H), 2.89 (dd, J = 17.0, 4.6 Hz, 1H), 2.73 (m, 1H), 2.65 (m, 2H), 1.38 (s, 9H).

Fmoc-Glu(OtBu)Cys(trt)Asp(OtBu)-OMe

Fmoc-Cys(trt)Asp(OtBu)-OMe (5.19 mmol, 4.00 g) was dissolved in 10 ml dry CH_2Cl_2. 1-Octanethiol (51.9 mmol, 9.04 ml) and DBU (0.52 mmol, 78 μl) were added, and the reaction was stirred for 15 hr at room temperature under Ar. After evaporation of the solvent, the resulting product was purified by flash chromatography eluting with a step gradient ranging from 2% to 50% EtOAc/CH_2Cl_2. H-Cys(trt)Asp(OtBu)-OMe (2.09 g, 73%) was obtained as a fine white powder. H-Cys(trt)Asp(OtBu)-OMe, (3.65 mmol, 2.00 g), Fmoc-Glu(OtBu)-OH (4.02 mmol, 1.71 g), EDC·HCl (4.38 mmol, 0.84 g), and HOBt·hydrate (4.38 mmol, 0.67 g) were dissolved in 10 ml dry CH_2Cl_2 and were cooled to 0ºC. DIEA (4.02 mmol, 0.71 ml) was added, and the reaction was stirred for 5 hr at room temperature. The usual workup and chromatography (acetone:CH_2Cl_2/1:20) yielded Fmoc-Glu(OtBu)Cys(trt)Asp(OtBu)-OMe (3.04 g, 87%) as a white powder. ^{1}H-NMR (400 MHz) δ 7.76 (d, J = 7.6 Hz, 2H) 7.56 (t, J = 7.2 Hz, 2H), 7.40 (m, 8H), 7.28 (m, 8H), 7.18 (m, 3H), 6.90 (d, J = 8.4 Hz, 1H), 6.61(d, J = 7.6 Hz, 1H), 5.84 (d, J = 6.4 Hz, 1H), 4.72 (m, 2H), 4.35 (d, J = 7.2 Hz, 2H), 4.15 (m, 2H), 4.04 (m, 1H), 3.67 (s, 3H), 2.82 (m, 2H), 2.67 (dd, J = 17.0 and 4.8 Hz, 1H), 2.57 (dd, J = 13.2 and 5.2 Hz, 1H), 2.40 (m, 1H), 2.30 (m, 1H), 2.03 (m, 1H), 1.88 (m, 1H), 1.44 (s, 9H), 1.40 (s, 9H).

Ac-Glu(OtBu)Cys(trt)Asp(OtBu)-OMe

Fmoc-Glu(OtBu)Cys(trt)Asp(OtBu)-OMe (0.31 mmol, 300 mg) was dissolved in 1 ml dry CH_2Cl_2. 1-Octanethiol (3.14 mmol, 546 μl) and DBU (0.031 mmol, 30 μl) were added, and the reaction was stirred for 16 hr at room temperature. The resulting product was purified by flash chromatography eluting with a step gradient ranging from 2% to 50% EtOAc/CH_2Cl_2. H-Glu(OtBu)Cys(trt)Asp(OtBu)-OMe (163 mg, 72%) was obtained as a fine white powder. H-Glu(OtBu)-Cys(trt)Asp(OtBu)-OMe (0.27 mmol, 198 mg) was dissolved in 3 ml dry CH_2Cl_2. Acetic anhydride (2.70 mol, 257 μl) was added to the reaction and was followed by DIEA (0.82 mmol, 114 μl), and the reaction was stirred for 1 hr at room temperature under Ar. The usual workup

and recrystallization of the crude product from CH_2Cl_2 yielded Ac-Glu(OtBu)Cys(trt)Asp(OtBu)-OMe (163 mg, 78%) as a white powder. ^{1}H-NMR (400 MHz) δ 7.42 (m, 6H) 7.30 (m, 6H), 7.21 (m, 3H), 6.86 (d, J = 8.4 Hz, 1H), 6.70 (d, J = 7.6 Hz, 1H), 5.53 (d, J = 6.8 Hz, 1H), 4.70 (m, 1H), 4.33 (m, 1H), 4.01 (m, 1H), 3.67 (s, 3H), 2.84 (dd, J = 16.8 and 5.2 Hz, 1H), 2.77 (dd, J = 13.2 and 8.0 Hz, 1H), 2.67 (dd, J = 16.8 and 4.8 Hz, 1H), 2.58 (dd, J = 12.8 and 5.2 Hz, 1H), 2.40 (m, 1H), 2.28 (m, 1H), 2.03 (m, 1H), 1.97 (s, 3H), 1.88 (m, 1H) 1.43 (s, 9H), 1.40 (s, 9H). ESI mass spectrum: Calcd (MNa^+) 798.35; Found 798.52.

Ac-GluCysAsp-OMe, 1

Ac-Glu(OtBu)Cys(trt)Asp(OtBu)-OMe was deprotected in a cocktail of H_2O, TIPS, and TFA (2.5:2.5:95) for 5 hr. The reaction mixture was concentrated with N_2 and precipitated with cold Et_2O. The precipitate was dissolved in 10% acetonitrile in H_2O, and it was reduced with DTT (10 mM) for 1 hr with stirring at 37ºC. Pure deprotected product was isolated as a white solid by reversed-phase C18 HPLC (1 cm × 30 cm, 5 μ) by using 0.1% TFA/H_2O and a linear gradient of CH_3CN. ESI mass spectrum: Calcd (MH^+) 420.12; Found 420.16.

NB-Glu(OtBu)Cys(trt)Asp(OtBu)-OMe, 3

H-Glu(OtBu)Cys(trt)Asp(OtBu)-OMe (0.22 mmol, 163 mg), 5-norbornene-*exo*-carboxylic acid (0.24 mmol, 34 mg), TBTU (0.24 mmol, 78 mg), and HOBt·hydrate (0.08 mmol, 13 mg) were dissolved in 2 ml dry CH_2Cl_2. DIEA (0.24 mmol, 43 μl) was added, and the reaction was stirred for 1 hr at room temperature. The usual workup and chromatography (acetone:CH_2Cl_2/1:20) yielded **3** (144 mg, 76%) as a white powder. ^{1}H-NMR (400 MHz) δ 7.41 (m, 6H) 7.29 (m, 6H), 7.21 (m, 3H), 6.94 (d, J = 8.4 Hz, 1H), 6.73 (m, 1H), 6.67 (m, 1H), 6.11 (m, 1H), 6.02 (m, 1H), 4.72 (m, 1H), 4.29 (m, 1H), 4.04 (m, 1H), 3.67 (s, 3H), 2.92 (m, 1H), 2.83 (m, 3H), 2.70 (m, 1H), 2. 48 (m, 2H), 2.29 (m, 1H), 2.02 (m, 2H), 1.88 (m, 4H), 1.64 (d, J = 7.2 Hz, 1H), 1.44 (d, J = 5.6 Hz, 9H), 1.41 (s, 9H), 1.27 (m, 2H). ^{13}C-NMR (400 MHz) δ 27.15, 27.21, 28.23, 28.28, 30.72, 30.77, 32.19, 32.24, 33.70, 33.77, 37.48, 41.78, 41.81, 44.77, 46.57, 46.63, 47.24, 47.39, 49.10, 52.39, 52.44, 52.69, 53.54, 53.64, 67.40, 81.43, 81.76, 127.11, 128.28, 128.29, 129.79, 136.08, 136.24, 138.34, 138.47, 144.58, 169.67, 169.94, 171.05, 171.36, 171.37, 173.68, 173.69, 176.58.

Cbz-Ser(tBu)Ala-OMe

H-Ala-OMe·HCl (27.20 mmol, 3.80 g), Cbz-Ser(tBu)-OH (29.91 mmol, 8.84 g), EDC·HCl (32.64 mmol, 6.26 g), and HOBt·hydrate (32.64 mmol, 5.00 g) were dissolved in 25 ml dry CH_2Cl_2 and were cooled to 0ºC. DIEA (29.91 mmol, 5.30 ml) was added, and the reaction was stirred for 12 hr at room temperature. The usual workup and chromatography (acetone:CH_2Cl_2/1:20) yielded Cbz-Ser(tBu)Ala-OMe (7.81 g, 76%) as a white powder. ^{1}H-NMR (400 MHz) δ 7.34 (m, 5H), 5.73 (m, 1H), 5.12 (m, 2H), 4.57 (m, 1H), 4.23 (m, 1H), 3.81 (m, 1H), 3.74 (s, 3H), 3.38 (t, J = 8.4 Hz, 1H), 1.40 (d, J = 7.2 Hz, 3H), 1.21 (s, 9H).

Cbz-Glu(OtBu)Ser(tBu)Ala-OMe

Cbz-Ser(tBu)Ala-OMe (1.62 mmol, 616 mg) was dissolved in 3 ml MeOH. 10% Pd/C (0.16 mmol, 17 mg) was added, and the reaction was stirred for 3 hr at room temperature under H_2. After filtration of the catalyst with celite, the resulting amine product was used without further purification. H-Ser(tBu)Ala-OMe (1.62 mmol, 400 mg), Cbz-Glu(OtBu)-OH (1.79 mmol, 604 mg), TBTU (1.34 mmol, 430 mg), and HOBt·hydrate (0.45 mmol, 69 mg) were dissolved in 3 ml dry CH_2Cl_2. DIEA (2.60 mmol, 460 μl) was added, and the reaction was stirred for 12 hr at room temperature. The usual workup and chromatography (acetone:CH_2Cl_2/1:20) yielded **8** (627 mg, 68%) as a white powder. ^{1}H-NMR (400 MHz) δ 7.33 (m, 6H) 7.01 (d, J = 6.8, 1H), 5.72 (d, J = 6.4 Hz, 1H), 5.10 (m, 2H), 4.56 (q, 1H), 4.43 (m, 1H), 4.23 (m, 1H), 3.81 (m, 1H), 3.73 (s, 3H), 3.36 (t, J = 7.6 Hz, 1H), 2.38 (m, 2H), 2.12 (m, 1H), 1.95 (m, 1H), 1.43 (s, 9H), 1.39 (d, J = 7.2 Hz, 3H), 1.21 (s, 9H).

NB-Glu(OtBu)Ser(tBu)Ala-OMe, 4

Cbz-Glu(OtBu)Ser(tBu)Ala-OMe (0.53 mmol, 300 mg) was dissolved in 3 ml MeOH. 10% Pd/C (0.053 mmol, 6 mg) was added, and the reaction was stirred for 2 hr at room temperature under H_2. After filtration of the catalyst with celite, the resulting amine product was used without further purification. H-Glu(OtBu)Ser(tBu)Ala-OMe (0.51 mmol, 220.0 g), 5-norbornene-*exo*-carboxylic acid (0.56 mmol, 78 mg), TBTU (0.56 mmol, 180 mg), and HOBt·hydrate (0.19 mmol, 29 mg) were dissolved in 3 ml dry CH_2Cl_2. DIEA (0.61 mmol, 108 μl) was added, and the reaction was stirred for 3 hr at room temperature. The usual workup and chromatography (acetone:CH_2Cl_2/2:10) yielded **4** (226 mg, 74%) as a white powder. ^{1}H-NMR (400 MHz) δ 7.38 (t, J = 8.0 Hz, 1H) 7.02 (t, J = 7.4 Hz, 1H), 6.82 (d, J = 5.6 Hz, 1H), 6.12 (m, 2H), 4.56 (q, 1H), 4.44 (m, 1H), 4.38 (m, 1H), 3.86 (m, 1H), 3.73 (s, 3H), 3.37 (m, 1H), 2.96 (m, 1H), 2.91 (m, 1H), 2.47 (m, 1H), 2.37 (m, 1H), 2.13 (m, 1H), 2.07 (m, 1H), 2.00 (m, 1H), 1.90 (m, 1H), 1.65 (m, 1H), 1.45 (d, J = 4.0 Hz, 9H), 1.41 (dd, J = 7.2 and 0.8 Hz, 3H), 1.35 (m, 2H), 1.19 (d, J = 4.8 Hz, 9H) ^{13}C-NMR (400 MHz) δ 18.30, 27.47, 27.52, 28.23, 30.62, 30.79, 32.25, 41.74, 41.76, 44.62, 44.67, 46.51, 46.57, 47.22, 47.37, 48.38, 48.41, 52.45, 52.47, 53.24, 53.87, 53.89, 61.48, 74.13, 74.18, 81.32, 81.33, 136.12, 138.40, 169.86, 169.88, 171.35, 171.38, 173.07, 173.62, 176.54, 176.55.

ROMP

The procedure detailed below for polymer $\mathbf{3}_{10}$ is representative of the procedure followed for synthesis of all of the homopolymers and the random copolymer. Scale, yield, and spectra are presented for each of the individual polymers. The number of ligands (n) is based on the monomer:catalyst ratio used in the synthesis and confirmed by integration in the ^{1}H-NMR spectra.

3₁₀

NB-Glu(OtBu)Cys(trt)Asp(OtBu)-OMe **3** (82 μmol, 70 mg) was dissolved in 100 μl CH_2Cl_2/MeOH (3/1). To the reaction was added oven-dried LiCl (1.2 mmol, 51 mg) and (H_2IMes)(PCy_3)Cl_2Ru=CHPh (8 μmol, 7 mg) dissolved in 50 μl CH_2Cl_2/MeOH (3/1) and an additional 250 μl CH_2Cl_2/MeOH (3/1). The reaction was stirred for 3 hr. Ethyl vinyl ether (1 ml) was added to quench the reaction, and the mixture was stirred for an additional 40 min. After removing the solvent, the residue was dissolved in CH_2Cl_2. The solution was washed three times with H_2O, dried with Na_2SO_4, concentrated by rotary evaporation, and precipitated with cold Et_2O. The product was isolated by centrifugation and dried. Crude protected polymer was deprotected with TFA/TIPS/H_2O (95/2.5/2.5) for 5 hr. The reaction mixture was concentrated with N_2 and was precipitated with cold Et_2O. The precipitate was collected by centrifugation. Polymer was dissolved in H_2O (1 ml) at pH 6 and reduced with 10–20 mM tris(2-carboxyethyl)phosphine (TCEP) for 2 hr at 37ºC. Reduced polymer was isolated by precipitation with 1 N HCl (200 μl). Residual TCEP was removed by repeated washing of the precipitate with H_2O (3 × 1 ml). $\mathbf{3}_{10}$, a yellowish-white solid, was collected (41 mg, 90%), dried, and stored at −20ºC. ^{1}H-NMR (400 MHz, D_2O) δ 7.24 (m) 5.34 (m), 4.65–4.05 (with max at 4.61, 4.42, 4.23), 3.61 (br s), 2.90–2.29 (with max at 2.80, 2.58, 2.45, 2.25), 2.22–1.45 (with max at 2.142, 1.86, 1.78), 1.18 (br s).

3₃

NB-Glu(OtBu)Cys(trt)Asp(OtBu)-OMe **3** (82 μmol, 70 mg) and (H_2IMes)(3-Br-pyr)$_2Cl_2$Ru=CHPh (27 μmol, 24 mg) in a total volume of 400 μl yielded $\mathbf{3}_3$ as a brownish-white solid (30 mg, 82%). ^{1}H-NMR (500 MHz, D_2O) δ 7.26 (m) 5.35 (m), 4.65–4.01 (with max at 4.55, 4.26, 4.04), 3.24 (br s), 2.90–2.29 (with max at 2.81, 2.51), 2.22–1.45 (with max at 2.12, 1.93, 1.78), 1.19 (m).

3₆

NB-Glu(OtBu)Cys(trt)Asp(OtBu)-OMe **3** (82 μmol, 70 mg) and (H_2IMes)(3-Br-pyr)$_2Cl_2$Ru=CHPh (14 μmol, 12 mg) in a total volume of 400 μl yielded $\mathbf{3}_6$ as a brownish-white solid (45 mg, 95%). ^{1}H-NMR (500 MHz, D_2O) δ 7.26 (m) 5.45–5.10 (with max at 5.36, 5.29, 5.26), 4.65–4.05 (with max at 4.59, 4.45, 4.27), 3.64 (br s), 2.90–2.45 (with max at 2.83, 2.63), 2.22–1.45 (with max at 2.21, 1.94, 1.84, 1.61), 1.21 (m).

3₇₀

NB-Glu(OtBu)Cys(trt)Asp(OtBu)-OMe **3** (17 μmol, 15 mg) and (H_2IMes)(PCy_3)Cl_2Ru=CHPh (0.17 μmol, 0.15 mg) in a total volume of 150 μl CH_2Cl_2/MeOH (3/1) yielded a yellowish-white solid (8 mg, 80%). ^{1}H-NMR (400 MHz, D_2O) δ 7.20 (m), 5.23 (m), 4.44–4.09 (with max at 4.39, 4.08), 3.67 (br s), 3.22 (s), 3.15–1.45 (with max at 2.95, 2.80, 2.10, 1.91, 1.81, 1.60), 1.38–1.79 (with max at 1.23, 1.15, 0.90).

4₁₀

NB-Glu(OtBu)Ser(tBu)Ala-OMe **4** (38 μmol, 21 mg) and (H_2IMes)(P-Cy_3)Cl_2Ru=CHPh (13.8 μmol, 3.3 mg) in a total volume of 200 μl CH_2Cl_2/MeOH (3/1) yielded $\mathbf{4}_{10}$ as a brownish-white solid (10 mg, 67%). ^{1}H-NMR (600 MHz, D_2O) δ 4.29 (m), 5.23 (br, s), 4.29 (m), 4.00

(m), 3.65 (br, s), 3.20 (s), 3.10–2.30 (with max at 2.80, 2.45), 2.25–1.40 (with max at 2.10, 1.90, 1.79, 1.45), 1.20 (m), 1.00 (m).

4_{70}

NB-Glu(OtBu)Ser(tBu)Ala-OMe **4** (47 μmol, 26 mg) and (H_2IMes)(P-Cy_3)Cl_2Ru=CHPh (0.47 μmol, 0.40 mg) in a total volume of 200 μl CH_2Cl_2/MeOH (3/1) yielded $\mathbf{4_{70}}$ as a brownish-white solid (12 mg, 63%). ^{1}H-NMR (600 MHz, D_2O) δ 7.20 (m), 5.80–5.20 (m), 3.45 (br, s), 2.2–1.4 (with max at 2.19, 1.99, 1.68), 1.38–0.80 (with max at 1.23, 1.15).

$3_8/4_{72}$

NB-Glu(OtBu)Cys(trt)Asp(OtBu)-OMe **3** (12 μmol, 10 mg), NB-Glu(Ot-Bu)Ser(tBu)Ala-OMe **4** (106 μmol, 58 mg), and (H_2IMes)(PCy_3)Cl_2Ru=CHPh (1.17 μmol, 0.99 mg) in a total volume of 400 μl CH_2Cl_2/MeOH (3/1) yielded $\mathbf{3_8/4_{72}}$ as a yellowish-white solid (36 mg, 73%). ^{1}H-NMR (600 MHz, D_2O) δ 7.22 (m) 5.45–5.10 (with max at 5.34, 5.23, 5.16), 4.65 (br s), 4.39–4.05 (with max at 4.31, 4.04), 3.75 (br s), 3.63 (br s), 2.85 (m), 2.48 (m), 2.22–1.41 (with max at 2.13, 1.90, 1.81, 1.60), 1.40–1.00 (with max at 1.31, 1.23, 1.12), 0.92 (br s).

$3_2'$, $3_2'$-$4_7'$, $3_2'$-$4_7'$-$3_2'$, 3_2-4_7-3_2

In three separate flasks, A, B, and C, peptide **3** (23 μmol, 20 mg) was dissolved in 100 μl CH_2Cl_2/MeOH (3/1). Then, oven-dried LiCl (1.2 mmol, 51 mg) and (H_2IMes)(3-Br-pyr)$_2Cl_2$Ru=CHPh (12 μmol, 10 mg) dissolved in 50 μl CH_2Cl_2/MeOH (3/1) were added to each flask. The reactions were stirred for 1.5 hr. To flask A, ethyl vinyl ether (2 ml) was added, and the mixture was stirred for 40 min to quench the reaction yielding $\mathbf{3_2'}$. To flasks B and C, peptide **4** (82 μmol, 45 mg) dissolved in 250 μl CH_2Cl_2/MeOH (3/1) was added, and the reactions were stirred for 1.5 hr. Ethyl vinyl ether (2 ml) was added to flask B, and the mixture was stirred for 40 min to yield $\mathbf{3_2'\text{-}4_7'}$. Then, peptide **3** (23 μmol, 20 mg) dissolved in 250 μl CH_2Cl_2/MeOH (3/1) was added to flask C, and the reaction was stirred for 2 hr. Ethyl vinyl ether (2 ml) was added to quench the reaction, and the mixture was stirred for an additional 40 min to yield $\mathbf{3_2'\text{-}4_7'\text{-}3_2'}$. For each reaction, TLC was used to confirm the complete disappearance of monomer before addition of the next monomer. After removing the solvent from each of the flasks, the residues were dissolved separately in CH_2Cl_2. The solutions were washed three times with H_2O and dried with Na_2SO_4, and the products $\mathbf{3_2'}$, $\mathbf{3_2'\text{-}4_7'}$, and $\mathbf{3_2'\text{-}4_7'\text{-}3_2'}$ were precipitated with cold Et_2O. The precipitates were isolated by centrifugation and dried. Each of the polymers was analyzed by gel permeation chromatography by using a Phenogel column (5μ, 300 × 4.60 mm, linear mixed bed, 100–10^6 MW range). Elution was performed at 0.3 ml/min with 10% MeOH in CH_2Cl_2. Narrowly dispersed polystyrene standards from Aldrich were used as molecular weight calibrants. The number-averaged and weighted average molecular weights were calculated from the chromatogram to determine the polydispersity index (PDI).

3_2-4_7-3_2

Crude protected polymer $\mathbf{3_2'\text{-}4_7'\text{-}3_2'}$ was deprotected with TFA/TIPS/H_2O (95/2.5/2.5) for 5 hr. The reaction mixture was concentrated with N_2, and the polymer was precipitated with cold Et_2O and isolated by centrifugation. The polymer was dissolved in H_2O (1 ml) at pH 6 and was reduced with 10–20 mM TCEP for 2 hr at 37ºC. Deprotected polymer was isolated by precipitation with 1 N HCl (200 μl). Residual TCEP was removed by repeated washing with H_2O (3 × 1 ml). $\mathbf{3_2\text{-}4_7\text{-}3_2}$, a yellowish-white solid (40 mg, 88%), was collected, dried, and stored at −20ºC. ^{1}H-NMR (500 MHz, D_2O) δ 7.26 (m) 5.35 (m), 4.40–4.01 (with max at 4.35, 4.27, 4.22, 4.06, 4.04), 3.77 (br s), 3.65 (br s), 3.25 (br s), 2.90–2.29 (with max at 2.85, 2.51), 2.22-1.45 (with max at 2.16, 1.93, 1.84, 1.62), 1.34 (br s), 1.26–1.02 (with max at 1.25, 1.15), 0.94 (br s).

Assay for Thiol Oxidation

5,5′-dithiobis(2-nitrobenzoic acid) (DTNB) was prepared as a 5 mM stock solution in 100 mM potassium phosphate buffer solution (pH 7.2), containing 0.1 mM EDTA, and was stored in the dark at 4ºC. All polymers were fully reduced with TCEP, washed three times with deionized water, and dissolved in aqueous ammonium hydroxide solution (pH 7.2). Aliquots of polymer (< 10 μl) were added to M16 (without BSA or phenol red) to a final volume of 100 μl and were incubated at 37ºC. The final concentrations of polymer were 100, 75, and 50 μM, and 9 aliquots were prepared at each concentration. At 5 min intervals for 45 min, 100 μl stock DTNB was added to a polymer aliquot, the solution was mixed, and the absorbance at 412 nm was measured. The concentration of free sulfhydryl remaining was determined by using $\varepsilon_{412} = 14{,}150\ M^{-1}cm^{-1}$ [34]. A standard curve for sulfhydryl concentration was prepared by using cysteine under the same conditions.

Isolation of Spermatozoa and Oocytes for IVF Assay

All experiments performed with mice were in accordance with the National Institute of Health and United States Department of Agriculture guidelines, and the specific procedures performed were approved by the Stony Brook University IACUC (protocol #0616). Sperm for the in vitro adhesion and fusion assay were isolated from the cauda epididymis and vas deferens of 8-month-old ICR retired male breeders (Taconic, NJ). Sperm were released from dissected cauda and vas deferens into 3% BSA M16-modified Krebs-Ringer medium. Released sperm were incubated at 37ºC, 5% CO_2 for 3 hr in the same medium to allow them to capacitate and acrosome react. Eggs were collected from the oviducts of 8- to 10-week-old superovulated female ICR mice (Taconic, NJ). Mice were superovulated by injecting 5 IU PMSG, followed 48–52 hr later by an injection of 10 IU hCG. A total of 14–16 hr after hCG injection, oviducts were removed from euthanized mice and were incubated in prewarmed M16 medium with 0.5% BSA. Cumulus-egg complexes were collected and transferred to 500 μl drops of medium containing 30 μg/ml hyaluronidase surrounded by mineral oil. After 5 min of incubation at 37ºC, 5% CO_2, cumulus-free metaphase II eggs (eggs with one polar body) were collected, transferred first to a 80 μl drop of medium, and then washed through six 40 μl drops of medium. Eggs were recovered for 1 hr before treating with Tyrode's acid. Zona pellucida of metaphase II eggs were removed by treating eggs with a 100 μl Tyrode's acid drop for 1 min at room temperature. Zona-free eggs were washed six times with 0.5% BSA medium and were recovered for 2 hr, then preloaded with HOECHST dye at 10 μg/ml for 30 min at 37ºC, 5% CO_2.

Inhibitor Assay

Before use, the polymers were fully reduced with 10 mM TCEP for 1–2 hr, precipitated with 1 N HCl, washed with water, and then redissolved in water adjusted to pH 7 with NH_4OH.

Zona-free eggs that had been loaded with Hoechst dye were washed and placed in 100 μl drops of 3% BSA M16 medium. Polymer solution was added (no more than 5 μl of stock solution) and incubated with eggs for 45 min prior to sperm addition. Capacitated and acrosome-reacted sperm were added to eggs at a final concentration of 1–5 × 10^5 sperm/ml. After 45 min at 37ºC, 5% CO_2, eggs were gently washed through six 40 μl drops of the M16 medium with 3% BSA. Eggs were mounted onto glass microscope slides, and sperm binding and fusion were scored by epi-fluorescence microscopy and DIC microscopy (NIKON Eclipse 400, 40×, 0.75 NA objective). Fusion was scored as the fluorescent labeling of sperm nuclei with HOECHST dye present in the preloaded eggs. Two measures of fusion were used: fertilization index (FI, mean number of fused sperm per egg) and fertilization rate (FR, percentage of eggs fused with at least one sperm). IC_{50}s were calculated by a three parameter fit (GRAFIT software) by the equation:

$$y = (100 - b)/\{1 + ([I]/IC_{50})\}^s, \quad (1)$$

where y is the percent FR or FI, b is the remaining percent fertilization after saturation with inhibitor, and s is the slope of the fit. Errors were reported as SEM.

Sperm Susceptibility to Polymer Assay

Sperm in 3% BSA M16-modified Krebs-Ringer medium were allowed to capacitate and acrosome react in a 37ºC humidified incubator with 5% CO_2 for 2 hr 30 min, then treated with 500 μM $\mathbf{3_{10}}$, $\mathbf{3_{70}}$, or $\mathbf{3_2\text{-}4_7\text{-}3_2}$ for 45 min. Control sperm were incubated in the same buffer. Samples were transferred to glass slides, and sperm motility and viability were checked by light microscope (NIKON TS-100, 10×, 0.25 NA objective). Only sperm that were still swimming actively were counted as viable and motile. In a second experiment, sperm were incubated for 45 min with 125 μM $\mathbf{3_2\text{-}4_7\text{-}3_2}$ in 3% BSA M16 buffer, or in medium alone. A total of 2 μl of the sperm incubation (1–5 × 10^5 sperm/ml) was transferred to a 100 μl M16 drop containing zona-free eggs. After 45 min, the eggs were analyzed for the number of sperm bound and fused as previously described in the assay.

Supplemental Data

Supplemental Data including NMR spectra are available at http://www.chembiol.com/cgi/content/full/13/3/251/DC1/.

Acknowledgments

This work was supported by funding from the National Institutes of Health (R01HD38519, N.S.S.), the National Science Foundation (REU CHE0139256, N.F.; CRIF CHE0131146, NMR), and an American Chemical Society Cope Scholar Award (N.S.S.).

Received: June 23, 2005
Revised: November 18, 2005
Accepted: December 16, 2005
Published online: March 24, 2006

References

1. Roberts, S.K., Konkar, S., and Sampson, N.S. (2003). Comparison of fertilinβ peptide-substituted polymers and liposomes as inhibitors of in vitro fertilization. ChemBioChem *4*, 1229–1231.
2. Evans, J.P. (2001). Fertilin β and other ADAMs as integrin ligands: insights into cell adhesion and fertilization. Bioessays *23*, 628–639.
3. Evans, J.P., Schultz, R.M., and Kopf, G.S. (1998). Roles of the disintegrin domains of mouse fertilins α and β in fertilization. Biol. Reprod. *59*, 145–152.
4. Primakoff, P., Hyatt, H., and Tredick-Kline, J. (1987). Identification and purification of a sperm surface protein with a potential role in sperm-egg membrane fusion. J. Cell Biol. *104*, 141–149.
5. Primakoff, P., and Myles, D.G. (2000). The ADAM gene family: surface proteins with adhesion and protease activity. Trends Genet. *16*, 83–87.
6. Seals, D.F., and Courtneidge, S.A. (2003). The ADAMs family of metalloproteases: multidomain proteins with multiple functions. Genes Dev. *17*, 7–30.
7. Myles, D.G., Kimmel, L.H., Blobel, C.P., White, J.M., and Primakoff, P. (1994). Identification of a binding site in the disintegrin domain of fertilin required for sperm-egg fusion. Proc. Natl. Acad. Sci. USA *91*, 4195–4198.
8. Pyluck, A., Yuan, R., Galligan, E., Jr., Primakoff, P., Myles, D.G., and Sampson, N.S. (1997). ECD peptides inhibit *in vitro* fertilization in mice. Bioorg. Med. Chem. Lett. *7*, 1053–1058.
9. Zhu, X., Bansal, N.P., and Evans, J.P. (2000). Identification of key functional amino acids of the mouse fertilin β (ADAM2) disintegrin loop for cell-cell adhesion during fertilization. J. Biol. Chem. *275*, 7677–7683.
10. Gupta, S., Li, H., and Sampson, N.S. (2000). Characterization of fertilinβ-disintegrin binding specificity in sperm-egg adhesion. Bioorg. Med. Chem. *8*, 723–729.
11. Evans, J.P., Schultz, R.M., and Kopf, G.S. (1995). Mouse sperm-egg plasma membrane interactions: analysis of roles of egg integrins and the mouse sperm homologue of PH-30 (fertilin) β. J. Cell Sci. *108*, 3267–3278.
12. Almeida, E.A.C., Huovila, A.P.J., Sutherland, A.E., Stephens, L.E., Calarco, P.G., Shaw, L.M., Mercurio, A.M., Sonnenberg, A., Primakoff, P., Myles, D.G., et al. (1995). Mouse egg integrin $\alpha_6\beta_1$ functions as a sperm receptor. Cell *81*, 1095–1104.
13. Gupta, S., and Sampson, N.S. (2001). Dimyristoylated peptides incorporated into liposomes are polyvalent fertilinβ mimics. Org. Lett. *3*, 3333–3335.
14. Yuan, R., Primakoff, P., and Myles, D.G. (1997). A role for the disintegrin domain of cyritestin, a sperm surface protein belonging to the ADAM family, in mouse sperm-egg plasma membrane adhesion and fusion. J. Cell Biol. *137*, 105–112.
15. Bronson, R.A., Fusi, F.M., Calzi, F., Doldi, N., and Ferrari, A. (1999). Evidence that a functional fertilin-like ADAM plays a role in human sperm-oolemmal interactions. Mol. Hum. Reprod. *5*, 433–440.
16. Gichuhi, P.M., Ford, W.C., and Hall, L. (1997). Evidence that peptides derived from the disintegrin domain of primate fertilin and containing the ECD motif block the binding of human spermatozoa to the zona-free hamster oocyte. Int. J. Androl. *20*, 165–170.
17. Choi, S.K. (2004). Synthetic Multivalent Molecules: Concepts and Biomedical Applications, First Edition (Hoboken, NJ: John Wiley and Sons, Inc.).
18. Kanai, M., Mortell, K.H., and Kiessling, L.L. (1997). Varying the size of multivalent ligands: the dependence of concanavalin A binding on neoglycopolymer length. J. Am. Chem. Soc. *119*, 9931–9932.
19. Strong, L.E., and Kiessling, L.L. (1999). A general synthetic route to defined, biologically active multivalent arrays. J. Am. Chem. Soc. *121*, 6193–6196.
20. Mammen, M., Choi, S.-K., and Whitesides, G.M. (1998). Polyvalent interactions in biological systems: implications for design and use of multivalent ligands and inhibitors. Angew. Chem. Int. Ed. Engl. *37*, 2754–2794.
21. Konkar, S., Gupta, S., and Sampson, N.S. (2004). Fertilinβ liposomes inhibit in vitro fertilization by steric blockage. Bioorg. Med. Chem. Lett. *14*, 1381–1384.
22. Roberts, K.S., and Sampson, N.S. (2004). A facile synthetic method to prepare fluorescently labeled ROMP polymers. Org. Lett. *6*, 3253–3255.
23. Chen, H., and Sampson, N.S. (1999). Mediation of sperm-egg fusion: evidence that mouse egg $\alpha_6\beta_1$ integrin is the receptor for sperm fertilinβ. Chem. Biol. *6*, 1–10.
24. Evans, J.P., Kopf, G.S., and Schultz, R.M. (1997). Characterization of the binding of recombinant mouse sperm fertilin β subunit to mouse eggs: evidence for adhesive activity via an egg β1 integrin-mediated interaction. Dev. Biol. *187*, 79–93.
25. Takahashi, Y., Yamakawa, N., Matsumoto, K., Toyoda, Y., Furukawa, K., and Sato, E. (2000). Analysis of the role of egg integrins in sperm-egg binding and fusion. Mol. Reprod. Dev. *56*, 412–423.
26. He, Z.-Y., Brakebusch, C., Fässler, R., Kreidberg, J.A., Primakoff, P., and Myles, D.G. (2003). None of the integrins known to be present on the mouse egg or to be ADAM receptors are essential for sperm-egg binding and fusion. Dev. Biol. *254*, 226–237.
27. Miller, B.J., Georges-Labouesse, E., Primakoff, P., and Myles, D.G. (2000). Normal fertilization occurs with eggs lacking the integrin $\alpha_6\beta_1$ and is CD9-dependent. J. Cell Biol. *149*, 1289–1296.
28. Trnka, T.M., and Grubbs, R.H. (2001). The development of L2X2Ru = CHR olefin metathesis catalysts: an organometallic success story. Acc. Chem. Res. *34*, 18–29.
29. Cairo, C.W., Gestwicki, J.E., Kanai, M., and Kiessling, L.L. (2002). Control of multivalent interactions by binding epitope density. J. Am. Chem. Soc. *124*, 1615–1619.
30. Maynard, H.D., Okada, S.Y., and Grubbs, R.H. (2001). Inhibition of cell adhesion to fibronectin by oligopeptide-substituted polynorbornenes. J. Am. Chem. Soc. *123*, 1275–1279.
31. Maynard, H.D., Okada, S.Y., and Grubbs, R.H. (2000). Synthesis of norbornenyl polymers with bioactive oligopeptides by ring-opening metathesis polymerization. Macromolecules *33*, 6239–6248.
32. Roberts, K.S., and Sampson, N.S. (2003). Increased polymer length of oligopeptide-substituted polynorbornenes using LiCl. J. Org. Chem. *68*, 2020–2023.
33. Bigler, D., Takahashi, Y., Chen, M.S., Almeida, E.A., Osbourne, L., and White, J.M. (2000). Sequence-specific interaction between the disintegrin domain of mouse ADAM 2 (fertilin β) and murine eggs. Role of the α(6) integrin subunit. J. Biol. Chem. *275*, 11576–11584.
34. Riener, C.K., Kada, G., and Gruber, H.J. (2002). Quick measurement of protein sulfhydryls with Ellman's reagent and with 4,4′-dithiodipyridine. Anal. Bioanal. Chem. *373*, 266–276.
35. Portoghese, P.S. (2001). From models to molecules: opioid receptor dimers, bivalent ligands, and selective opioid receptor probes. J. Med. Chem. *44*, 2259–2269.
36. Loidl, G., Groll, M., Musiol, H.J., Huber, R., and Moroder, L. (1999). Bivalency as a principle for proteasome inhibition. Proc. Natl. Acad. Sci. USA *96*, 5418–5422.
37. Loidl, G., Musiol, H.J., Groll, M., Huber, R., and Moroder, L. (2000). Synthesis of bivalent inhibitors of eucaryotic proteasomes. J. Pept. Sci. *6*, 36–46.
38. Love, J.A., Morgan, J.P., Trnka, T.M., and Grubbs, R.H. (2002). A practical and highly active ruthenium-based catalyst that effects the cross metathesis of acrylonitrile. Angew. Chem. Int. Ed. Engl. *41*, 4035–4037.